The 2013 World Congress on
Advances in Structural Engineering and Mechanics (ASEM13)
Jeju, Korea, September 8-12, 2013

Effects of uncertainty in aeroelastic coefficients on the buffeting response of a long-span bridge

*Dong-Woo Seo[1)], Luca Caracoglia[2)] and Ki-Tae Park[3)]

[1), 3)] *Structural Engineering Research Division, Korea Institute of Construction Technology*
2311, Daewha-dong, Goyang-si, Gyeonggi-do, 411-712, Republic of Korea
[2)] *Department of Civil and Environmental Engineering, Northeastern University, Boston, MA 02115, USA*
[1)] *dwseo@kict.re.kr*

ABSTRACT

This study discusses the implementation of a methodology for the wind-induced response of long-span bridges, including uncertainty in the aeroelastic input (i.e., flutter derivatives, FDs). FDs are the most important part of the loading and are estimated in a wind tunnel experiment. The simplified polynomial model ("model curves") for the FDs is applied, including variability coming from wind tunnel experiments, and is employed in the multi-mode buffeting analysis using Monte-Carlo simulations. In the proposed probabilistic setting one estimates the probability that a given threshold for the variance of the response is exceeded. This probability is later used, together with information on the probability of the wind velocity at a given site, to predict the expected value of the loss function due to the buffeting response of a 1200-meter suspension bridge.

1. INTRODUCTION

This paper describes the development of a methodology for predicting the buffeting response of a long-span bridge by Monte Carlo (MC) methods (Robert and Casella 2004; Tempo et al. 2005). In the standard buffeting analysis (labeled as the "deterministic case" in this work) the result is the value of the RMS dynamic response at a given wind speed. In the proposed probabilistic setting (labeled as

[1)] Research Specialist
[2)] Associate Professor
[3)] Research Fellow

"statistical case" in this work) one estimates the probability that a given threshold for the variance of the response is exceeded.

A Monte-Carlo-based methodology is implemented for predicting the buffeting bridge response and for evaluating the variability due to uncertainty in the FDs ("statistical buffeting" analysis) described in (Seo and Caracoglia 2012a). To accomplish these tasks, a second order polynomial model ("model curve") for the FD is utilized. The model curve is a second order polynomial description of the FDs where uncertainty is associated with coefficient of the polynomial. The coefficients of this polynomial are treated as random variables, whose probability distribution is conditional on reduced wind speed. For computational reasons in subsequent analysis, however, this dependency is neglected and the probability of these random variables is treated as independent of the reduced wind speed. For analysis purposes the first and second order statistics are estimated from experiments, treating all the wind speed data as part of the same population.

A numerical procedure for multi-mode buffeting response ("deterministic case") was initially developed and its accuracy was validated by comparing with more reliable data from the literature. In the standard multi-mode buffeting analysis, the power spectral density (PSD) of the buffeting loads needs to be computed. This step, carried out by numerical integration, is usually the "bottleneck" of the multi-mode buffeting analysis method in the modal space. MC methods were used to numerically compute the PSD of the buffeting loads and to derive the root-mean-square (RMS) dynamic response of a long-span bridge, details can be found in (Seo and Caracoglia 2012a).

Finally, the complete procedure (labeled as "MC-based methodology" in this paper), which includes the probabilistic setting, is presented and implemented to numerically evaluate for the probability of exceeding a set of pre-selected serviceability thresholds, selected according to the RMS response of the deck as a function of mean wind velocity and mean incident angle (skew wind). Such curves or surfaces were again derived by MC sampling for two simulation examples, based on the 1,200 m suspension bridge structure.

The MATLAB software environment was employed for coding purposes. The detailed flowchart of the MC-based methodology for "statistical buffeting" analysis, including the uncertainty in the FD.

2. MONTE-CARLO-BASED METHODOLOGY FOR BUFFETING ANALYSIS SCONSIDERING UNCERTAINTY IN THE FLUTTER DERIVATIVE ("STATISTICAL CASE")

A Monte-Carlo-based methodology is implemented for predicting the buffeting bridge response and for evaluating the variability due to uncertainty in the FDs simulated by MC sampling. To accomplish these tasks, the second order polynomial model ("model curve" in Eq. 1 and 2) for the FD is utilized, in which the

coefficients of the polynomial are random variables; more details can be found in (Seo and Caracoglia 2012a).

$$H_i^*\left(U_R\right) = C_j U_R^2 + C_{j+1} U_R, \qquad i = 1,...,4 \qquad j = 1,3,5,7 \qquad (1)$$

$$A_i^*\left(U_R\right) = D_j U_R^2 + D_{j+1} U_R. \qquad i = 1,...,4 \qquad j = 1,3,5,7 \qquad (2)$$

These parameters become C_j and C_{j+1} for H_i^*, D_j and D_{j+1} for A_i^*. The general form for all H_i^* and A_i^* derivatives can be expressed as in Eqs. (1–2) with i=1,…,4 and j=1,3,5,7. In Eq. (1), C_j and C_{j+1} are constant parameters of the model, which are assumed as random coefficients and can be related in a simple way to experimental errors. The mean values of C_j and D_j can be determined from the mean of experimental points, extracted at various wind speeds in wind tunnel; similarly, second-moment properties of C_j and D_j can be related to the variances of measured FDs; the coefficients of the polynomial are determined from statistical regression of the experimental data, described in a separate sub-section.

In the MC-based methodology for buffeting analysis, the numerical procedure re-calculates, at various wind speeds and skew wind angles, the buffeting loads by MC sampling for each of the 5,000 realizations (e.g., the flowchart presented in Fig. 1). The generalized power spectral density (PSD) of the buffeting loads is also calculated by MC sampling, where a double integration is needed.

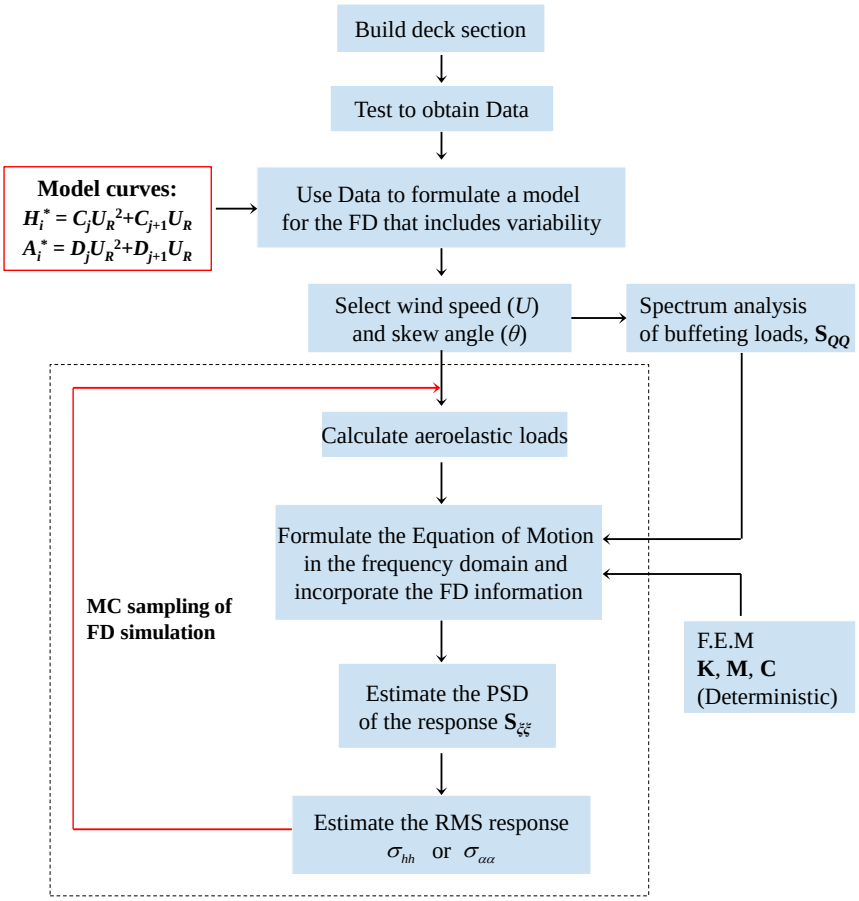

Note: The numerical procedure depicted in the box is repeated for N_{MC} times at various wind speeds and skew wind angles

Fig. 1 Flowchart describing the MC-based methodology for buffeting analysis

In the proposed probabilistic setting ("statistical buffeting case") one estimates the probability that a given threshold for the variance of the response is exceeded. There are two obvious formats to display the information that are useful in different ways. One way is to plot the RMS value of buffeting response at a given confidence level of not being exceeded. For example, the RMS value cab be presented for buffeting response as a function of wind speed at a given confidence level. More directly useful way for our purpose is to plot the probability of exceedance at a given fixed RMS value as a function of wind speed. This probability is designated as "threshold exceedance probability" (TEP) in this work, derived by using a MC-based methodology with 5,000 sampling points (e.g., the flowchart presented in Fig. 1) which projects the variability in the FD into the estimation of buffeting response. The concept of using TEP was adopted from seismic engineering field (i.e., "fragility").

Fragility analysis is a standardized methodology, utilized for performance-based structural design. As a general statement, fragility curves measure (or quantify) the overall structural vulnerability (Norton et al. 2008). The likelihood of structural damage due to different "demand levels" – mean wind velocity levels in the case of wind engineering – is usually expressed by a fragility curve (Saxena et al. 2000). A collection of these curves describes the (conditional) probability of exceedance of representative structural response indicators ("structural capacity"), corresponding to a specific feature of the dynamic response at a given wind velocity (Bashor and Kareem 2007; Ellingwood 2000; Filliben et al. 2002). A set of thresholds is usually selected to represent different levels of structural performance derived from such indicators. As an example, in the case of a building these indicators are either required or are prescribed by the designer, and can include inter-story drift ratios, maximum lateral drift, and acceleration levels for occupant comfort (Bashor and Kareem 2007; Filliben et al. 2002; Smith and Caracoglia 2011).

2.1 Description of the Bridge Example and RMS Threshold Levels ("Probabilistic Setting")

The suspension bridge model has a truss-type girder and replicates the behavior of the Golden Gate Bridge in San Francisco, California (USA) with main span l = 1,263 m, deck width B = 27.43 m. Frequencies, modal inertias, modal integrals, modal damping were adapted from previous studies (Jain et al. 1996); the contribution of moving deck and cables was included in the aeroelastic analyses.

The FDs H_i^* and A_i^* along with the static coefficients of lift and moment of the deck at an initial angle of attack α_0 = 0° were reproduced from (Jain et al. 1998); the FDs are shown in Fig. 2 as a function of reduced wind velocity $U_R = U/(nB)$, with U being the mean wind speed at deck level, n a frequency.

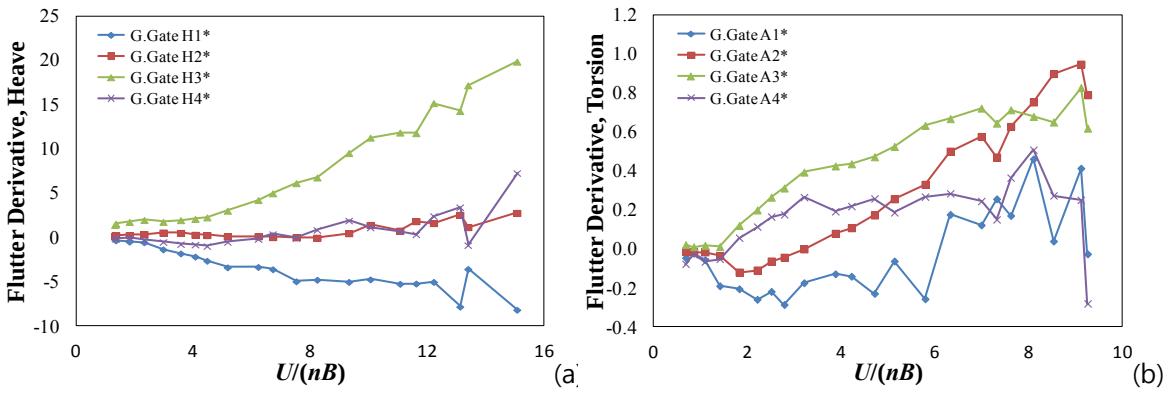

Fig. 2 Flutter derivatives used in conjunction with the 1200 m truss-type bridge model, derived from (Jain et al. 1996): (a) heave; (b) torsion.

This bridge example was selected for “threshold exceedance probability” (TEP) analysis, the same bridge model discussed in Section 4.2. Four-mode buffeting analysis was carried out by considering the first two vertical (v1 and v2) and torsional modes (t1 and t2); it has frequencies nv1 = 0.087 Hz and nv2 = 0.129 Hz, nt1 = 0.192 Hz and nt2 = 0.197 Hz. Simplified (sinusoidal-like) mode shapes.

The second order polynomial model (“model curve”) for flutter derivatives, proposed in Section 3.4 to approximately account for effects of measurement errors in the FD, was employed in the “statistical buffeting” analysis. Since eight flutter derivatives (H_1^*,…,H_4^* and A_1^*,…,A_4^*) are measured in wind tunnel as a function of the reduced speed, $U_R = U/(nB) = 2\pi/K$, experimental data are usually available at discrete points on the U_R (or K) axis. In the TEP analysis, the coefficients of the model curves for each flutter derivative were randomly perturbed to simulate the uncertainty in the FD.

The parameters of H_i^* and A_i^* were assumed as a set of uncorrelated gamma-type random variables. Description on the selection of this specific probability distribution may be found in (Seo and Caracoglia 2012a). The dispersion and shape parameters of the marginal probability of each variable were associated with mean and standard deviation estimates of H_i^* and A_i^*.

2.2 Multimode analysis and peak response estimation

The dynamic response of a long-span bridge due to wind loading can be modeled after the multi-mode approach in the frequency domain, for example discussed in Jones & Scanlan3. Buffeting forces per unit length can be described by quasi-steady theory. The analysis also included the effects of skew-wind angle since, in nature, the highest winds of record at a given site may be skew to the bridge Scanlan10. The multi-mode approach for wind direction orthogonal to the deck axis was therefore modified to account for relative directionality (mean-wind skew angle), as described in (Scanlan 1993).

Equation 3 (below) describes the modal force cross-spectra (modes i and j) as a function of the reduced frequency K, the generalized modal inertias I_i and the total deck length l. The cross PSD (power spectral density) of the generalized buffeting loading is obtained by double integration of the spectrum of the turbulence-induced loads, denoted as $S_F(x_A, x_B, K)$ in compact form, between two generic deck sections, x_A and x_B, which accounts for the mode shapes of i and j and partial span-wise correlation of the pressures (and loads):

$$S_{Q_i Q_j}(K) = \left(\frac{\rho B^4 l}{2U}\right)^2 \frac{1}{I_i I_j} \int_0^l \int_0^l S_F(x_A, x_B, K) \frac{dx_A}{l} \frac{dx_B}{l}. \tag{3}$$

From the previous equation the cross-PSD of the dynamic response can be evaluated by standard random vibration methods, with the ultimate goal being the evaluation of the RMS dynamic response. As an example, the cross-RMS dynamic response of *h* (heave) between sections *A* and *B* of the deck can be found through the PSD function of the vertical response S_{hh}, derived as explained in (Jones and Scanlan 2001) and from Equation (3), as:

$$\sigma_{hh}\left(x_A, x_B\right) = \sqrt{\int_0^\infty S_{hh}(x_A, x_B, K)dK}. \tag{4}$$

The equations above were exclusively reproduced from the multi-mode approach in order to highlight the need for a double integration in Equation (3), frequency by frequency, prior to estimation of RMS response in Equation (4). This operation may become computationally demanding and impractical in the context of statistical buffeting (Seo and Caracoglia 2012a). MC integration is used to reduce computational time and allow for subsequent fragility analysis.

Peak estimation via RMS response was also utilized. The peak value of *h* or *α*, the dynamic displacement or rotation of the generic deck section, can be determined by multiplying the RMS value by the peak effect factor (*g*). This factor was calculated through the equation proposed by (Davenport 1964), strictly valid for stationary Gaussian processes, as follows:

$$E\left[g\right] \cong \sqrt{2\log_e\left(\nu_{0,y}\hat{T}_0\right)} + \frac{0.577}{\sqrt{2\log_e\left(\nu_{0,y}\hat{T}_0\right)}}, \tag{5}$$

$$\nu_{0,y}^{+} = \frac{1}{2\pi}\frac{\sigma_{\dot{y}\dot{y}}}{\sigma_{yy}}, \tag{6}$$

where, σ_{yy} is used to designate generic RMS response (e.g., σ_{hh} for vertical response); $\sigma_{\dot{y}\dot{y}}$ is the generic RMS velocity; T_0 is a reference duration (averaging wind time) for estimation of peak crossings, usually equal to 10 minutes.

In order to evaluate the effect of wind-induced vibration on user comfort for bridge serviceability, RMS acceleration of the response and its peak value are more relevant than displacements or rotations for human perception. These quantities were calculated and applied in the cost analysis, discussed in the later section. For example, the cross-RMS acceleration $\sigma_{\ddot{h}\ddot{h}}$ can be derived from Equation (4); the peak accelerations $\ddot{h}(x)$ at deck section x can be found as:

$$\sigma_{\dot{h}\dot{h}}(x_A, x_B) = \sqrt{\int_0^\infty K^4 S_{hh}(x_A, x_B, K) dK}, \tag{7}$$

$$\hat{\ddot{h}}(x) = \sigma_{\ddot{h}\ddot{h}}(x, x) \cdot g. \tag{8}$$

2.3 Monte-Carlo-based fragility analysis

"Loss of performance" of the bridge (P_T) can be related to the probability of exceeding a threshold T, associated with the dynamic response feature *Y* (performance indicator) at a given deck section for mean wind speed U, wind incidence angle (θ) relative to the longitudinal axis. This approach enabled the analysis of the combined influence of wind directionality and velocity, as these should be more realistically used in serviceability analysis. "Fragility curves and surfaces" (Filiben et al. 2002; Grigoriu 2002) were derived as a function of *U* and θ for various threshold levels. Loss of performance of the bridge can be expressed as (Grigoriu 2002)

$$P_T = \int_{-180}^{180} \int_0^\infty P\left[Y > T \,|U = u, \Theta = \theta\right] f_{U\Theta}(u, \theta) du d\theta. \tag{9}$$

In Equation 9, the conditional probability function, denoted as *P*[], is the "fragility surface" (a fragility curve coincides with the case with θ=0°) and $f_{U\Theta}$ is the joint probability density function (PDF) between mean wind velocity (*U*) and wind incidence angle (θ) with respect to the longitudinal axis of the bridge; this angle is defined in the interval -180° ≤ θ ≤ 180° (θ=0°, 180° orthogonal to the bridge, θ=±90° parallel to the bridge).

2.4 Expected lifetime cost

Over a time period (*t*, in years), which may be the design life of a new bridge or the remaining life of an existing bridge, the expected total cost can be expressed as a function of t as follows (Wen and Kang 2001):

$$E\left[C(t)\right] = C_0 + E\left[\sum_{i=1}^{N(t)} \sum_{j=1}^{k} C_j e^{-\lambda t_i} P_j\right]. \tag{10}$$

In the previous equation, *E*[] denotes expected value; C_0 is the initial construction cost of the structure; *i* is an index describing each severe loading occurrence; $t_i \le t$ is the loading occurrence time of event "*i*", a random variable.

Moreover, $N(t)$ is the total number of wind damaging events over time t (another random variable, described by a Poisson counting process as suggested in Wen and Kang, 2001). The quantity C_j is the cost in present dollar value of j-th limit state being reached at time t_i of the loading occurrence; $e^{-\lambda t i}$ is the "discounted factor" (Wen and Kang 2001) of the "intervention" cost C_j over time t; λ is a constant discount rate per year; P_j is the probability of occurrence for limit state j (denoted as P_T in Eq. 9), which is assumed as a constant over time since no structural deterioration is anticipated in the context of serviceability limit states; the integer index k is the total number of limit states under consideration. The P_j probabilities must be found from the fragility surfaces, and are estimated from Equation (9) through the MC-based methodology in (Seo and Caracoglia 2012a). As suggested in (Wen and Kang 2001), the integer variable $N(t)$ can be approximated as a Poisson counting process.

In the specific prototype application under investigation four limit states were separately considered. As a consequence, Equation (10) was modified and adapted from its original form to obtain the expected value of maintenance and repair cost C_E, normalized with respect to the initial construction cost C_0 at t=0, as

$$C_E = \frac{E\left[C(t)-C_0\right]}{C_0} = \begin{cases} E\left[\sum_{i=1}^{N(t)} \varepsilon_1 e^{-\lambda t_i} P_1\right] & (j\text{=1 only,User comfort}) \\ E\left[\sum_{i=1}^{N(t)} \varepsilon_2 e^{-\lambda t_i} P_2\right] & (j\text{=2 only, Deformation, lower tolerance}) \\ E\left[\sum_{i=1}^{N(t)} \varepsilon_3 e^{-\lambda t_i} P_3\right] & (j\text{=3 only, Deformation, higher tolerance}) \end{cases} \tag{11}$$

In Eq. 11 the cost, associated with each limit state, is expressed as $\varepsilon_j C_0$ (j=1,2,3) with ε_j being the ratio of this cost relative to C_0. The expected value of intervention cost normalized to the initial construction cost in Equation 11, ε_j (j=1,2,3) will be later discussed along with the numerical example. In Equation 9 the expected value of the cost was found by categorizing the number of occurrences for wind events into "moderate wind storms" for serviceability and buffeting limit states from j=1 to j=3.

In particular, the number of occurrences for moderate wind storms $N(t)$ at time t was based on a Poisson counting Process with an annual occurrence rate, derived from the probability of annual wind speed maxima exceeding U=20 m/s, based on actual site winds in the proximity of the actual bridge; this is equal to 0.94 independent of direction θ. This wind speed value was chosen to reflect a minimum demand level, corresponding to a small but non-negligible deck vibration (e.g., vertical vibrations exceeding 0.27 m or 1/30 of the deck height D).

Table 1 shows the limit states employed in the cost analysis for the case study (shown for the vertical deck response only). Three thresholds for limit states (T_1 to T_3) were used in the cost analysis under buffeting response. The level T_1, associated with limit state j=1 and maximum vertical deck accelerations (or torsional accelerations), was selected as a user comfort level based on human perception. The thresholds associated with maximum vertical dynamic displacements (or torsional rotation) was sub-categorized as T_2 (limit state j=2) and T_3 (limit state j=3); T_2 is a more stringent level (lower tolerance) and T_3 is a less restrictive level (higher tolerance). In Table 1 the threshold T_1 was taken as 20 milli-g of peak deck vertical acceleration; T_2 and T_3 were taken as 1 m and 2 m of peak vertical deck oscillation, respectively; these simulate an unacceptable deformation in the bridge deck or superstructure during serviceability. The thresholds listed in Table 1 were employed in the fragility analysis for vertical vibrations; for torsional acceleration and peak deck rotations the same threshold levels as in Table 1 were used and normalized with respect to B/2 in order to be compatible with an equivalent vertical oscillation of the same order of magnitude (for example with T_1 being equal to 20 milli-g, T_2 equal to 1 m and T_3 equal to 2 m).

Table 1 Structural performance thresholds for vertical deck response (T_j).

Buffeting Thresholds (deck level)		
Human comfort (T_1, peak acceleration)	Lower Tolerance Deformation (T_2, peak displacement)	Higher Tolerance Deformation (T_3, peak displacement)
20 milli-g	1 m	2 m

3. FRAGILITY ANALYSIS CONSIDERING UNCERTAINTY IN THE FD

The wind data, used to estimate $f_U(U)$ and $f_\theta(\theta)$ given the assumption $f_{U\theta} = f_U.f_\theta$, was extracted from the historical records of a meteorological buoy close to the coast of California in San Francisco (USA), which is part of the NOAA (National Oceanic and Atmospheric Administration) system and National Data Buoy Center (NOAA Station 9414290, Latitude: 37.807 N, Longitude: 122.465 W, Shown in Fig. 4.20). This particular meteorological station was selected because the prototype full-scale application (Golden Gate Bridge) is located in proximity of the station. Data are available on-line from http://www.ndbc.noaa.gov/. Wind speeds and directions at this station are measured using an anemometer located 7.3 meters above mean sea level.

The annual wind speed maxima, obtained from the 16-year period, was fitted to an Extreme Value Type-I distribution with two parameters, i.e., scale equal to 30.0 and location equal to 9.6 (Simiu and Scanlan 1996). The distribution of the mean yaw-wind angle was based on a non-parametric model for the statistical distribution and derived from the histogram of the mean wind direction (azimuthal)

recorded by the sensor at elevation 7.3 m, postulating little effects of elevation on directionality. The azimuthal direction was later converted to yaw-wind angle by using actual orientation of the bridge axis.

In Fig. 3 three “fragility curves” (threshold exceedance probability curves), associated with the bridge model and based on flutter derivatives provided in (Jain et al. 1998), are presented. The fragility curves were calculated for both vertical and torsional response at the quarter span of the simulated bridge with an incident wind angle orthogonal to the bridge deck $\theta = 0°$.

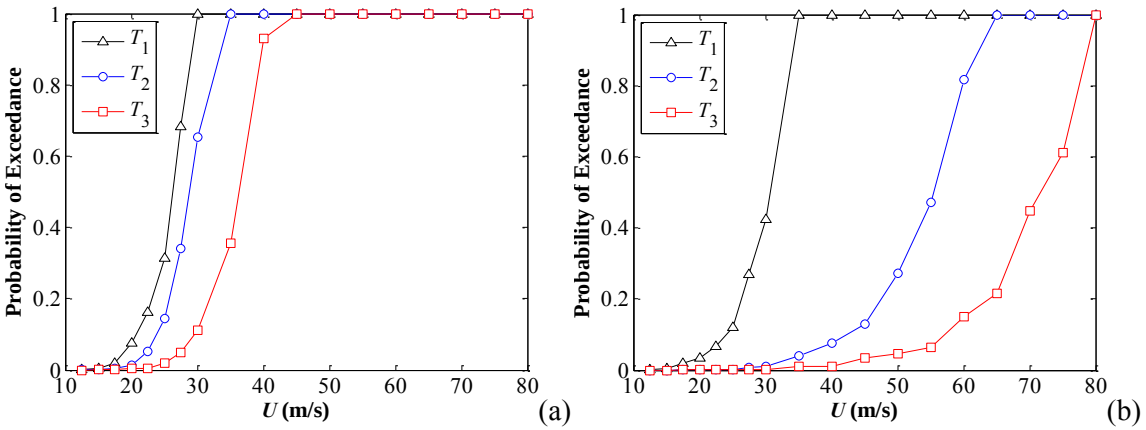

Fig. 3 Rescaled fragility curves of the peak dynamic response with respect to thresholds T_1, T_2, T_3 for the quarter-span deck section: (a) vertical response; (b) torsional response.

The curves in Fig. 3 were numerically computed by exclusively considering the buffeting response without the analysis of collapse probability influenced by the onset of flutter. This observation highlights the fact that wind load and fragility analysis should be “multi-hazard” to also account the probabilistic occurrences of flutter instability, by separating these events from buffeting vibrations.

The MC-based methodology for buffeting analysis numerically calculates the peak acceleration (T_1) and the peak displacements (T_2, T_3) of both vertical and torsional responses. As explained in (Seo and Caracoglia 2012a), at a given wind speed, since flutter may have occurred on a sub-set of events (statistically), the procedure can still find a finite peak displacement if one restricts the attention to the sub-set of events for which flutter has not occurred. Since the cost analysis (Eq. 9) focuses on the buffeting response only, it is necessary to “exclude” the events leading to flutter in the derivation of fragility curves and surfaces. Therefore, the approximate “rescaling” by applying Bayes’ Formula was utilized (as described in (Seo and Caracoglia 2012a)). The rescaled curves for thresholds T_1, T_2, T_3 are shown in Fig. 3. The “rescaling” requires the flutter probability to be evaluated; this was carried out numerically, details can be found in (Seo and Caracoglia 2012a).

Figs. 4 and 5 show the fragility surfaces for vertical and torsional response of the quarter-span deck section (*l*/4), based on flutter derivatives from Jain's data (Fig. 2) and corresponding to the thresholds in Table 1. The relative skew wind angle, varying from θ = –40° to θ = 40°, was exclusively analyzed.

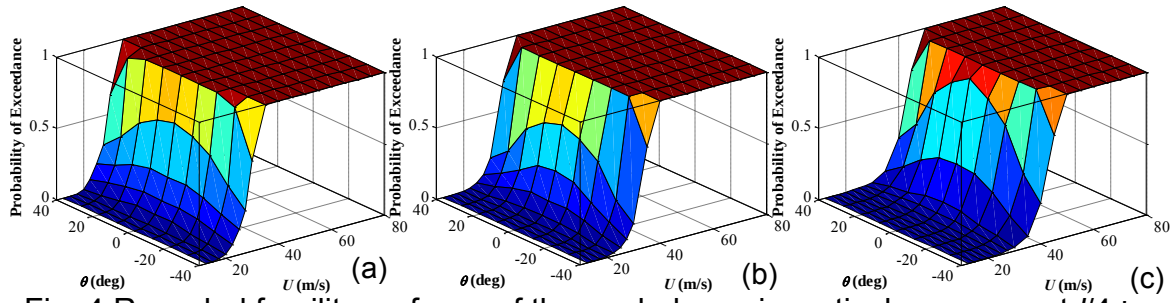

Fig. 4 Rescaled fragility surfaces of the peak dynamic vertical response at *l*/4 for various "intervention" thresholds using: (a) T_1=20 milli-g; (b) T_2=1m; (c) T_3=2m.

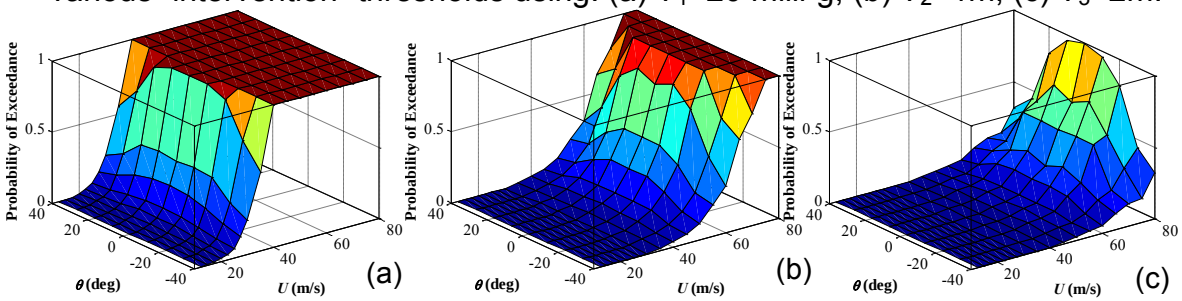

Fig. 5 Rescaled fragility surfaces of the peak dynamic (normalized to B/2) torsional response at l/4 for various intervention thresholds: (a) T_1=0.007rad/s^2; (b) T_2=0.036rad; (c) T_3=0.073rad.

4. LIFETIME EXPECTED INTERVENTION COST ANALYSIS - NUMERICAL RESULTS

4.1 Estimation of the Limit-State Probabilities P_j from fragility Analysis

In this section, an example of expected lifetime cost analysis is described. Table 2 shows the probabilities of each limit state (P_j), calculated for the buffeting intervention thresholds described in Table 1 as in Equation 7 (with P_T being the performance loss probability of the T limit state). Both the case, which considers variability in the FD, and without variability were examined. As outlined earlier, the threshold level T_1 for user comfort and two levels for deck deformation were investigated: T_2 a more conservative intervention threshold level and T_3 a less restrictive level. Preliminary inspection of the results revealed that the limit state probabilities P_2 and P_3 for torsional response for the specific bridge example and the section at *l*/4 are zero (i.e., orders of magnitude smaller) for 0<U<80 m/s when

variability in FD is neglected (i.e., for “deterministic buffeting”). This remark confirmed that “deterministic buffeting” analysis underestimates the loss function significantly without requiring further investigation. When variability in FDs is considered, the torsional results are still well below the vertical case. Therefore, the results of the fragility analysis for vertical deck response were exclusively used later in the cost analysis.

Table 2 Probabilities of each damage state (Pj) due to buffeting response based on the structural performance thresholds (T = Tj).

Using Jain’s FD Data		Probabilities of Damage State, $P[Y>T]$		
		P_1	P_2	P_3
Vertical Response	Without variability in FD	0.60E-03	2.30E-03	1.50E-03
	With variability in FD	3.00E-03	2.80E-03	2.30E-03
Torsional Response	Without variability in FD	2.00E-03	0.00E+00	0.00E+00
	With variability in FD	2.70E-03	1.30E-03	4.00E-04

As described in previous sections and in Table 2 the threshold T_1 used in the cost analysis corresponds to peak deck acceleration; also, T_2 and T_3 correspond to the peak vertical oscillation requiring intervention for serviceability. The probabilities in Table 2 for the three thresholds (T_1, T_2 and T_3) were computed from the fragility surfaces in Figs. 4 and 5 and Eq. 9.

In Eq. 7 the probability density functions of the wind speed $f_U(U)$ and mean wind direction $f_\theta(\theta)$ were obtained from the “raw” wind data, assuming U and θ as independent random variables, recorded at the meteorological station close to the benchmark bridge. The probability density function of annual 10-minute averaged wind velocity maxima, shown in Fig. 6, was derived from the NOAA annual wind speed maxima over a 16-year period (1996-2011) and was employed to evaluate $f_U(U)$. A detailed description of the station and data resources can also be found in (Seo and Caracoglia 2012b). Derivation of the probability density functions of the annual wind speed maxima (f_U) and mean skew wind angle (f_θ) enabled the estimation of P_j (j=1,2,3) in Eq. (11) after fragility analysis.

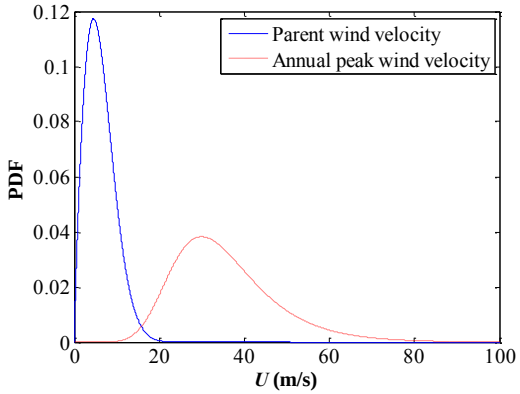

Fig. 6 PDFs of mean wind velocity and annual maxima ("annual peak wind velocity") of mean wind velocity, data from (NOAA).

4.2 Expected Intervention Cost

Probability mass function (PMF) was utilized to investigate how the cost varies with a random arrival time of each wind event (t_i and in Eq. 11). The arrival time of the events was modeled as a uniform random variable between 0 and t with the counting of the total number of Poisson's events, $N(t)$. Monte-Carlo sampling was employed to estimate the PMF of the relative maintenance and repair cost, $(C(t)-C_0)/C_0$, using 500 repeated Monte-Carlo realizations and five percent discount rate/year (λ). Intervention criteria can be found in Table 1 (T_j, j=1,2,3); a time projection of 60 years was used; probabilities of exceeding the limit states were taken from the P_j values in Table 2 (j=1,2,3). The ratios of this cost relative to construction cost C_0 were chosen to be 20% for all intervention levels ε_1, ε_2, and ε_3, as a first approximation

The results of the cost analysis are summarized in Figures 7 and 8. The compilation of these figures was based on two different intervention criteria: Figure 7 for user comfort (i.e., P_1), and Figure 8 for disproportionate deformation in the deck (i.e., P_2 or P_3). Five markers (black +, blue ◊, cyan ○, magenta □, and green Δ) and one red solid line are shown in the stem plots (Fig. 7). Each point on the stem plots represents a probability range: + probability between 0 and 0.2, ◊ between 0.2 and 0.4, ○ between 0.4 and 0.6, □ between 0.6 and 0.8, Δ less than 1.0. The solid line describes the evolution of the C_E (Eq. 9) expected relative cost, as a function of time, derived from the PMF stem plots.

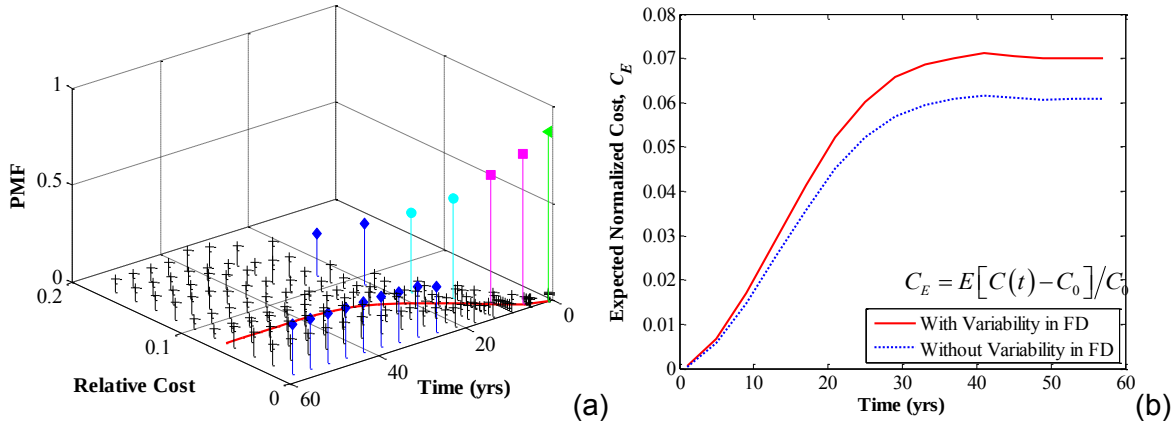

Fig. 7 Intervention costs normalized to the initial construction cost for user comfort level threshold T_1=20 milli-g over time: (a) 3D PMF (probability mass function stem plot); (b) 2D expected normalized cost.

Figure 7(b) shows the results of the cost analysis due to buffeting response using Jain's FD data. For an intervention level threshold T_1 of 20 milli-g of maximum vertical acceleration (for user comfort) the loss function estimated without considering the uncertainty in the FDs was approximately 15% lower for exposure times of 40 years or more, as indicated in Figure 7(b). For an intervention level threshold T_2 of 1 m of maximum vertical deformation (lower tolerance), the underestimation was approximately 22% for 40 years of exposure or longer, as in Figure 8(a). For the higher tolerance case T_3 of 2 m of maximum vertical deformation the underestimation proved to be 53% for 40 years of exposure or longer, with a progressive reduction trend with lower exposure times similar to that for the lower threshold.

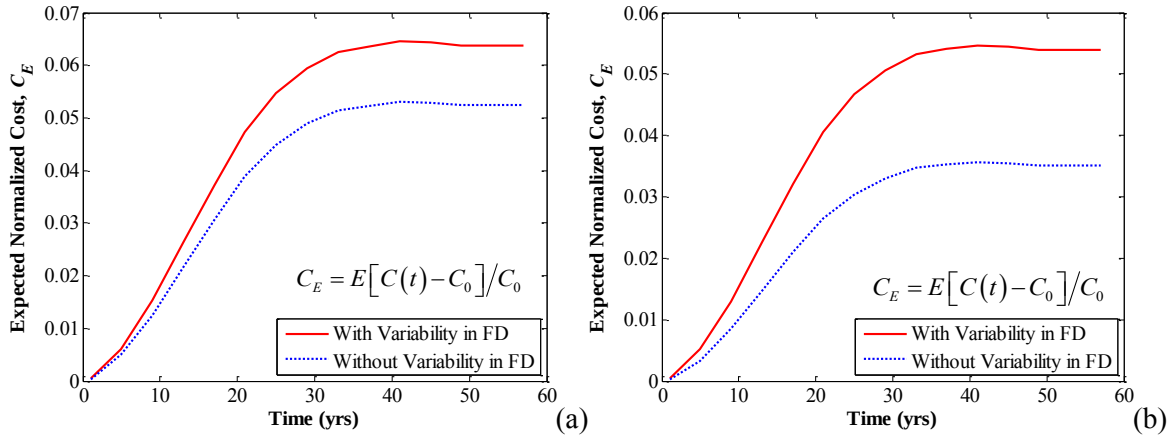

Fig. 8 Expected intervention costs normalized to the initial construction cost due to deformation in deck: (a) lower tolerance case (T_2=1m); (b) higher tolerance case (T_3=2m).

5. DISCUSSION

The cost analysis result showed that the expected value of the loss function due to the buffeting response of a suspended bridge, a function proportional to the cost associated with interventions needed to ensure safety, is affected by the variability of the FDs in a manner that depends on the time of exposure and one the threshold used to decide on the need for intervention (maintenance or repair).

For user comfort level threshold (T_1) of 20 milli-g of maximum vertical acceleration the loss function estimated without considering the uncertainty in the FDs was approximately 15% low for exposure times of 40 years or more. For exposure times less than 40 years the underestimation decreased (approximately) linearly for both cases, down to zero for zero exposure time. For the intervention level threshold with lower tolerance (T_2) of 1m of maximum vertical deck deformation the underestimation was 22% for 40 years of exposure or longer.

For higher tolerance case, T_3 of 2m of maximum vertical deformation, the underestimation proved to be 53% for 40 years of exposure or longer, with a reduction trend with exposure similar to that for the lower threshold. This result showed that, at least for the specific bridge example under investigation, consideration of the FD variability in the estimation of the loss function is important when the threshold for intervention is relatively high.

ACKNOWLEDGEMENTS

This research is based upon work supported by the National Science Foundation of the United States (NSF), Award No. 0600575, between 2006 and 2010. The first and third authors would also like to thank the Korea Institute of Construction Technology (KICT) for the partial support. Any opinions, findings, and conclusions or recommendations are those of the writers and do not necessarily reflect the views of these agencies.

REFERENCES

Bashor, R., and Kareem, A. (2007). "Probabilistic performance evaluation of buildings: An occupant comfort perspective." *12th International Conference on Wind Engineering (12-ICWE)*, Cairns, Australia, July 1-6, 2007, 1335-1342.

Davenport, A. G. (1964). "Note on the distribution of the largest value of a random function with application to gust loading." *Journal of the Institution of Civil Engineers*, 24, 187-196.

Ellingwood, B. R. (2000). "LRFD: Implementing structural reliability in professional practice." *Engineering Structures*, 22(2), 106-115.

Filiben, J. J., Gurley, K., Pinelli, J.-P., and Simiu, E. (2002). "Fragility curves, damage matrices, and wind induced loss estimation." *Third International Conference on Computer Simulation in Risk Analysis and Hazard Mitigation*, Sintra, Portugal, 119-126.

Filliben, J. J., Gurley, K., Pinelli, J.-P., and Simiu, E. (2002). "Fragility curves, damage matrices, and wind induced loss estmation." *Third International Conference on 'Computer Simulation in Risk Analysis and Hazard Mitigation'*, Sintra, Portugal, 119-126.

Grigoriu, M. (2002). *Stochastic calculus. Applications in Science and Engineering*, Birkhäuser, Boston, MA, USA.

Jain, A., Jones, N. P., and Scanlan, R. H. (1996). "Coupled aeroelastic and aerodynamic response analysis of long-span bridges." *Journal of Wind Engineering and Industrial Aerodynamics*, 60(1-3), 69-80.

Jain, A., Jones, N. P., and Scanlan, R. H. (1998). "Effect of modal damping on bridge aeroelasticity." *Journal of Wind Engineering and Industrial Aerodynamics*, 77-78, 421-430.

Jones, N. P., and Scanlan, R. H. (2001). "Theory and full-bridge modeling of wind response of cable-supported bridges." *Journal of Bridge Engineering, ASCE*, 6(6), 365-375.

NOAA. National Data Buoy Center.

Norton, T., Abdullah, M., M. , and Stephens, D. (2008). "Proposed methodology for performance-based vulnerability assessment of wind-excited tall buildings." *Fourth International Conference on 'Advances in Wind and Structures (AWAS'08)'*, Techno-Press, Korea, ISBN 978-89-89693-23-9-98530, Jeju, South Korea, 1228-1246.

Robert, C. P., and Casella, G. (2004). *Monte Carlo statistical methods (2nd ed.)*, Springer Science, New York, New York, USA.

Saxena, V., Deodatis, G., Shinozuka, M., and Feng, M. Q. (2000). "Development of fragility curves for multi-span reinforced concrete bridges." *International Conference on Monte Carlo Simulation*, Balkema, Principality of Monaco.

Scanlan, R. H. (1993). "Bridge buffeting by skew winds in erection stages." *Journal of Engineering Mechanics*, 119(2), 251-269.

Seo, D.-W., and Caracoglia, L. (2012a). "Statistical buffeting response of flexible bridges influenced by errors in aeroelastic loading estimation." *Journal of Wind Engineering and Industrial Aerodynamics*, 104–106(0), 129-140.
Seo, D.-W., and Caracoglia, L. (2012b). "Statistical buffeting response of flexible bridges influenced by errors in aeroelastic loading estimation." *Journal of Wind Engineering and Industrial Aerodynamics*, 104-106, 129-140.
Simiu, E., and Scanlan, R. H. (1996). *Wind effects on structures*, 3rd edition Ed., John Wiley and Sons, New York, NY, USA.
Smith, M. A., and Caracoglia, L. (2011). "A Monte Carlo based method for the dynamic “fragility analysis” of tall buildings under turbulent wind loading." *Engineering Structures*, 33(2), 410-420.
Tempo, R., Calafiore, G., and Dabbene, F. (2005). *Randomized algorithms for analysis and control of uncertain systems*, Springer-Verlag London Limited, London.
Wen, Y. K., and Kang, Y. J. (2001). "Minimum building life-cycle cost design criteria. I: Methodology." *Journal of Structural Engineering*, 127(3), 330-337.